Supplementary Information for:

Elucidation of superionic conduction in K_2NiF_4-type Ba–Li oxyhydride from first-principles molecular dynamics study

Jun Haruyama,[*,†] *Fumitaka Takeiri,*[†,‡] *Genki Kobayashi,* [†,§] *and Osamu Sugino*[‖]

[†]Solid State Chemistry Laboratory, Pioneering Research Institute (PRI), RIKEN, 2-1 Hirosawa, Wako, Saitama 351-0198, Japan

[‡]Department of Chemistry, Kindai University, 3-4-1 Kowakae, Higashiosaka, Osaka 577-8502, Japan

[§]Department of Electrical Engineering and Bioscience, School of Advanced Science and Engineering, Waseda University, 3-4-1 Okubo, Shinjuku-ku, Tokyo 169-8555, Japan

[‖]The Institute for Solid State Physics, The University of Tokyo, 5-1-5 Kashiwanoha, Kashiwa, Chiba 277-8581, Japan

Corresponding Author

*jun.haruyama@riken.jp

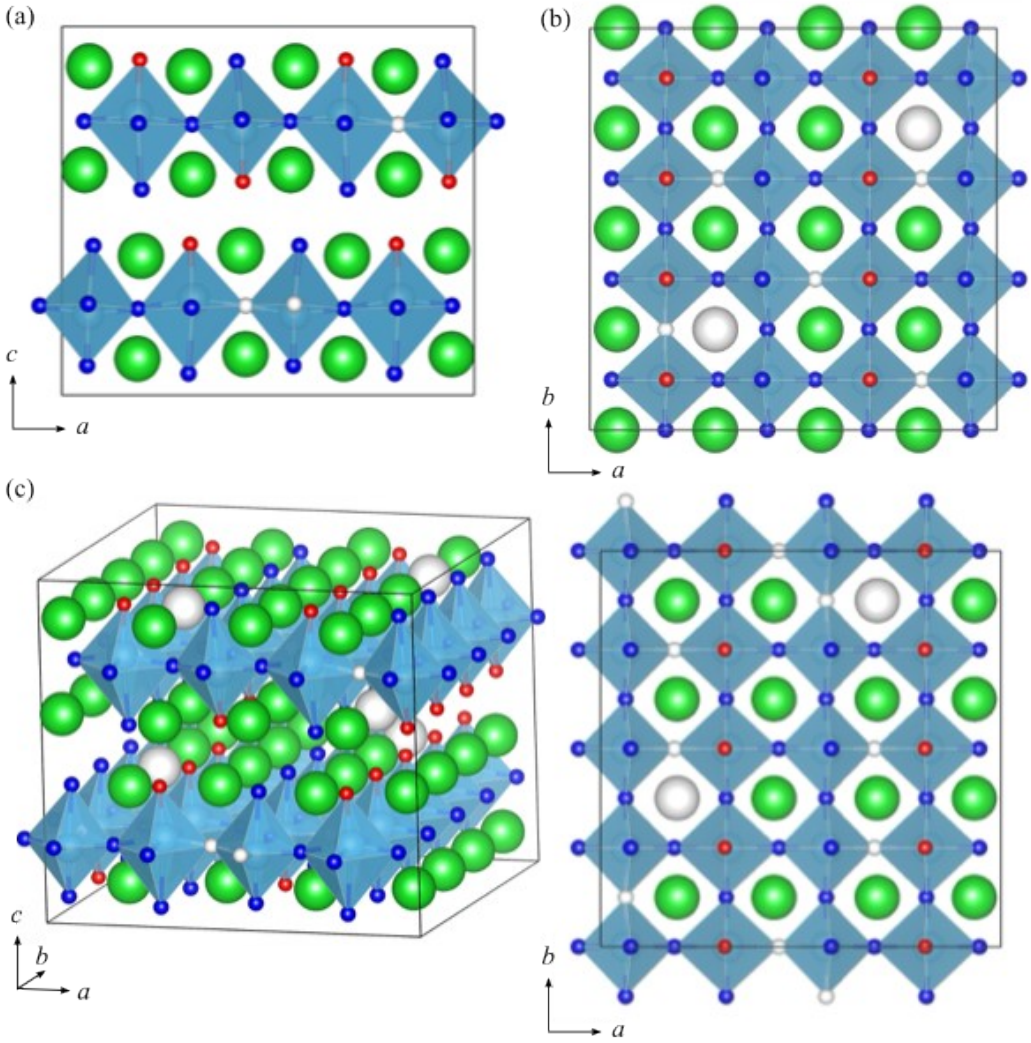

Figure S1. (a) Crystal structures of β-like $Ba_{56}Li_{32}H_{88}O_{28}$: (a) side, (b) top (bottom and top layers), and (c) oblique views. Ba, Li H, and O atoms are depicted as green, light blue, blue, and red spheres, respectively. V_H and V_{Ba} are depicted as small and big white spheres, respectively. Blue octahedrons and black lines represent the LiX_6 (X = H, O, and V_H) unit and periodic unit cell, respectively.

Table S1. Number of atoms, composition ratios, and numbers of H_{eq} and Ba vacancies in composition change models.

Number of atoms	Composition ratio	V_H	V_{Ba}
$Ba_{56}Li_{32}H_{88}O_{28}$	$Ba_{1.75}LiH_{2.75}O_{0.88}$	12	8
$Ba_{57}Li_{32}H_{90}O_{28}$	$Ba_{1.78}LiH_{2.81}O_{0.88}$	10	7
$Ba_{58}Li_{32}H_{90}O_{29}$	$Ba_{1.81}LiH_{2.81}O_{0.91}$	9	6

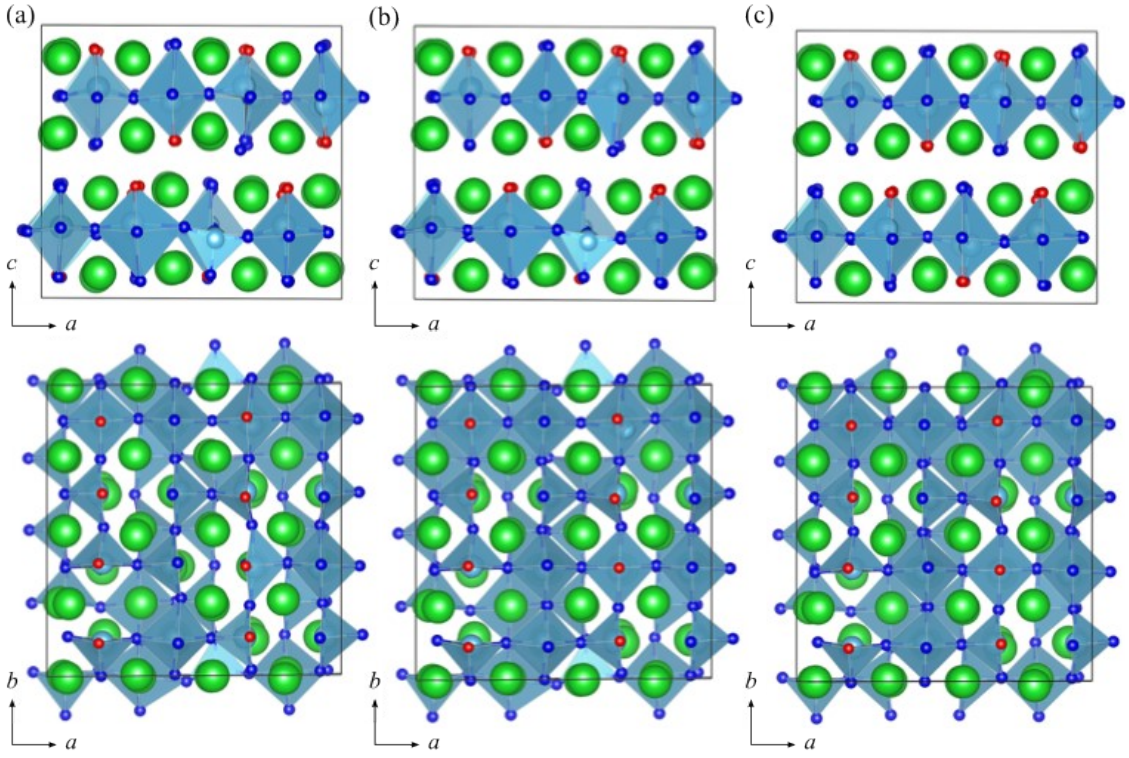

Figure S2. (a) Optimized structures of β-like (a) $Ba_{56}Li_{32}H_{88}O_{28}$, (b) $Ba_{57}Li_{32}H_{90}O_{28}$ ($1V_{Ba}$ and $2V_H$ in $Ba_{56}Li_{32}H_{88}O_2$ are occupied), and (c) $Ba_{58}Li_{32}H_{90}O_{29}$ ($1V_{Ba}$ and $1V_H$ are occupied and $1H_{ap}$ is replaced $1O_{ap}$ in $Ba_{57}Li_{32}H_{90}O_{28}$).

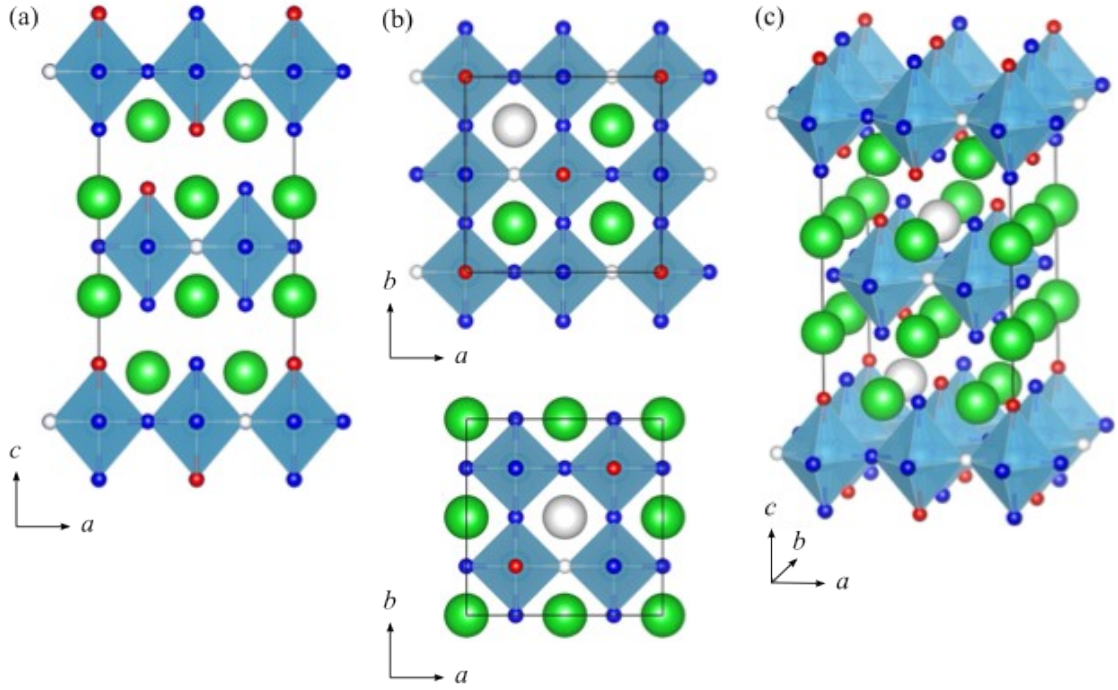

Figure S3. (a) Crystal structure of δ-like $Ba_{14}Li_8H_{22}O_7$: (a) side, (b) top (bottom and middle layers), and (c) aerial views.

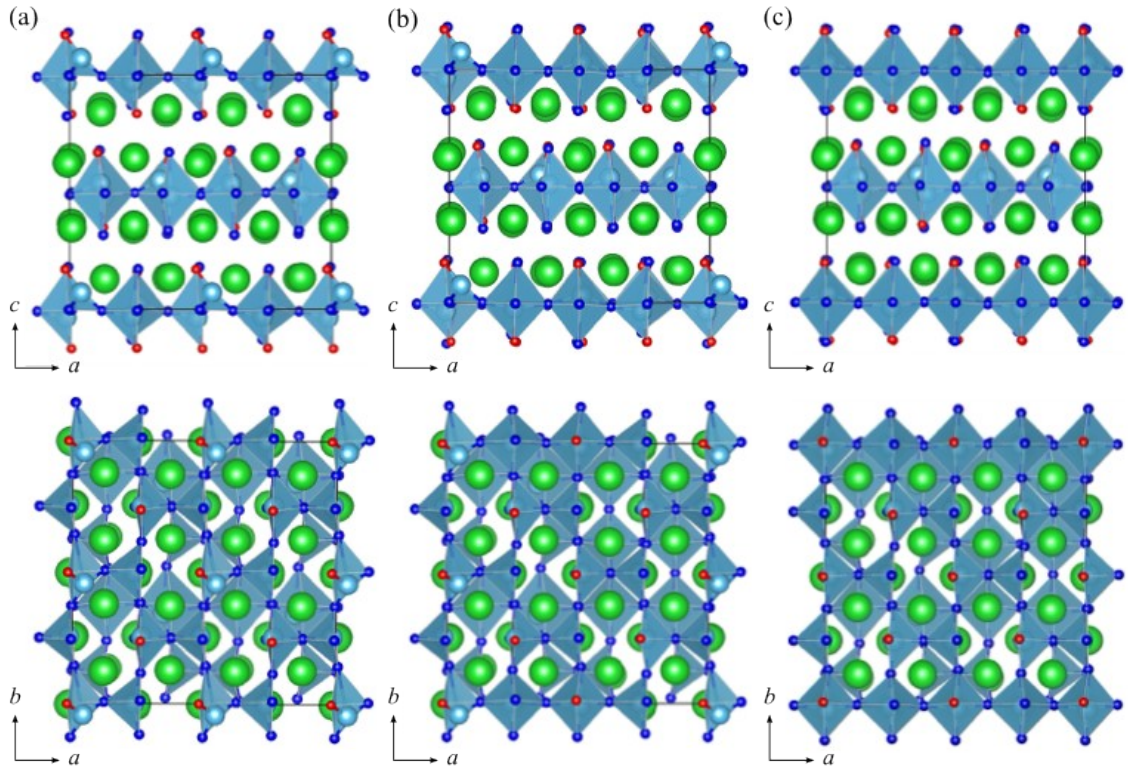

Figure S4. (a) Optimized structures of δ-like (a) $Ba_{56}Li_{32}H_{88}O_{28}$ (2×2×1 duplication cell of $Ba_{14}Li_8H_{22}O_7$), (b) $Ba_{57}Li_{32}H_{90}O_{28}$, and (c) $Ba_{58}Li_{32}H_{90}O_{29}$.

Table S2. Mimicked phases, numbers of atoms, optimized lattice constants (a, b, and c), and calculated bandgaps E_{gap} of composition change models.

phase	Number of atoms	a [Å]	b [Å]	c [Å]	E_{gap} [eV]
β-like	$Ba_{56}Li_{32}H_{88}O_{28}$	15.82	15.74	14.47	2.69
	$Ba_{57}Li_{32}H_{90}O_{28}$	15.81	15.76	14.45	2.60
	$Ba_{58}Li_{32}H_{90}O_{29}$	15.83	15.78	14.38	2.59
δ-like	$Ba_{56}Li_{32}H_{88}O_{28}$	15.724	15.999	14.395	2.43
	$Ba_{57}Li_{32}H_{90}O_{28}$	15.754	15.967	14.332	2.34
	$Ba_{58}Li_{32}H_{90}O_{29}$	15.775	15.939	14.301	2.23

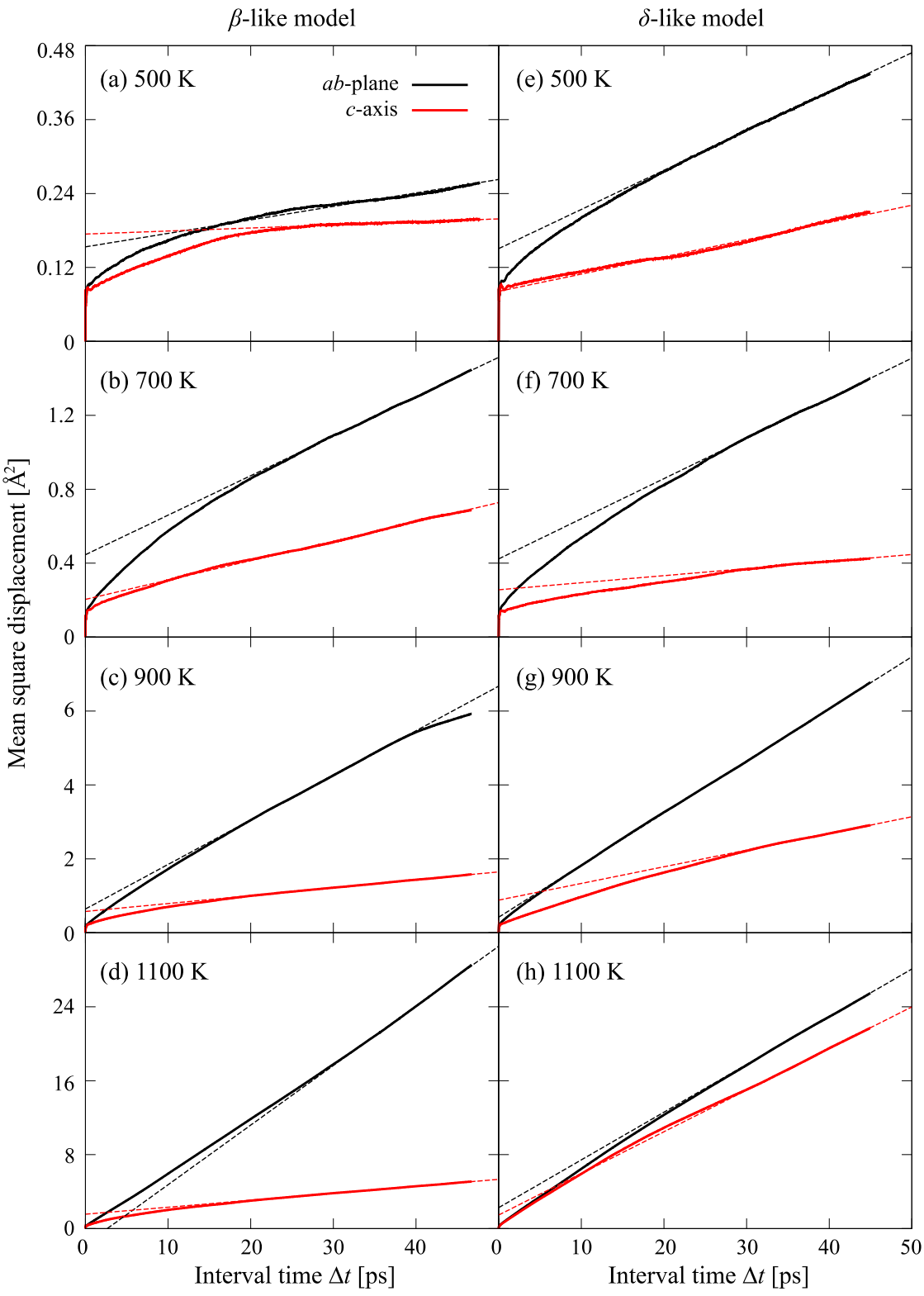

$\sum_i^N \left\langle \left| \mathbf{r}_i(t+\Delta t) - \mathbf{r}_i(t) \right|^2 \right\rangle$

Figure S5. Mean square displacements of H, , obtained by (a–d) β- and (e–h) δ-like models at controlled temperatures. Black and red solid lines represent *ab*-plane and *c*-axis

components, respectively. Dashed lines indicate fitted line slope by linear interpolation.

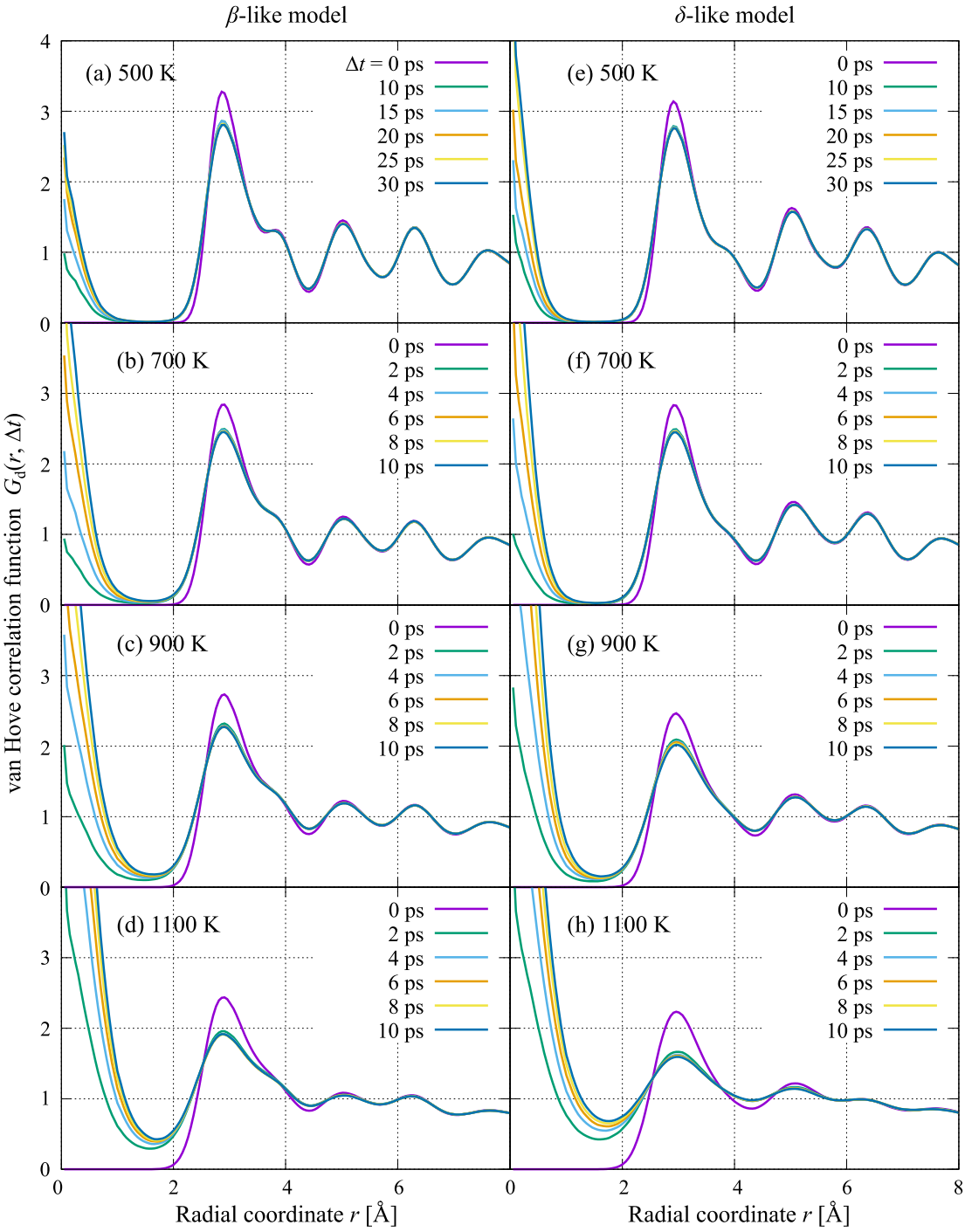

Figure S6. van Hove correlation function $G_d(r, \Delta t)$ as a function of radial coordinate r obtained by (a–d) β- and (e–h) δ-like models at controlled temperatures. Colors correspond to the extracted interval times Δt as shown in subset.

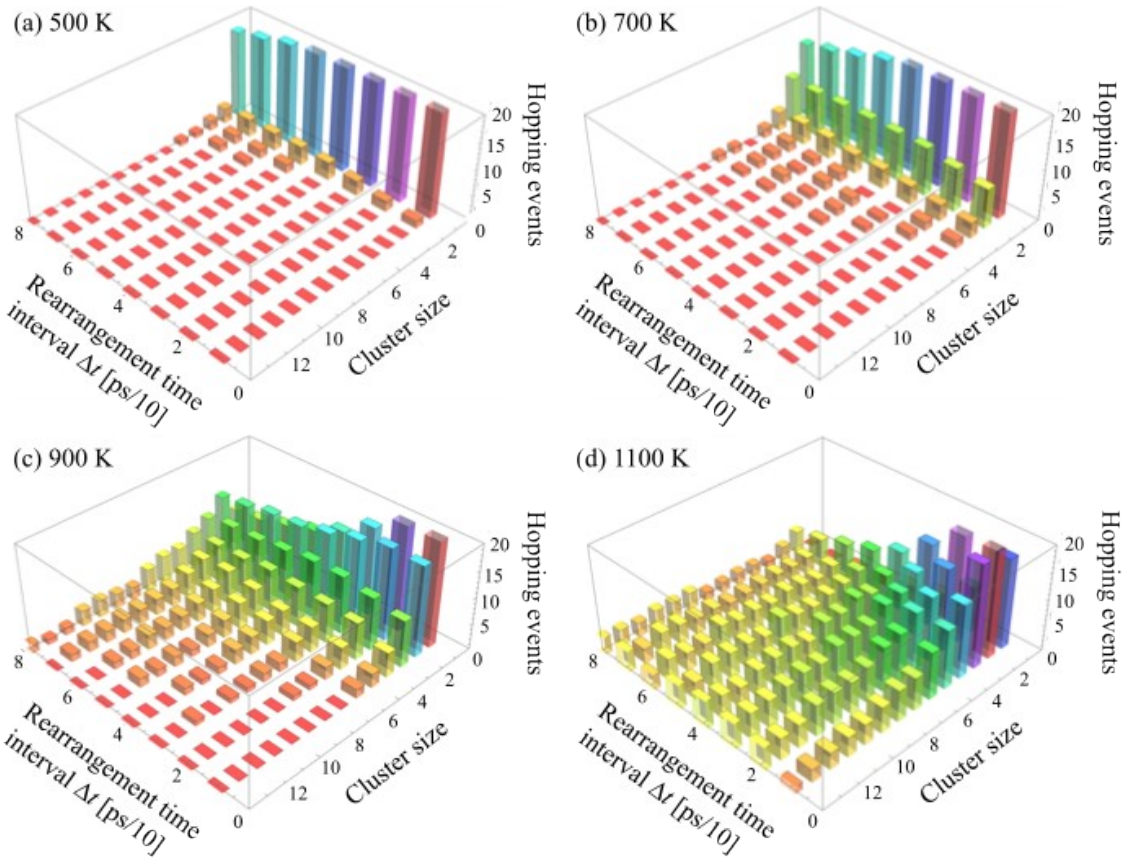

Figure S7. Aerial views of hopping events as functions of cluster size and rearrangement time interval obtained at the controlled temperatures of (a) 500, (b) 700, (c) 900, and (d) 1100 K. Colors of rods correspond to their height.

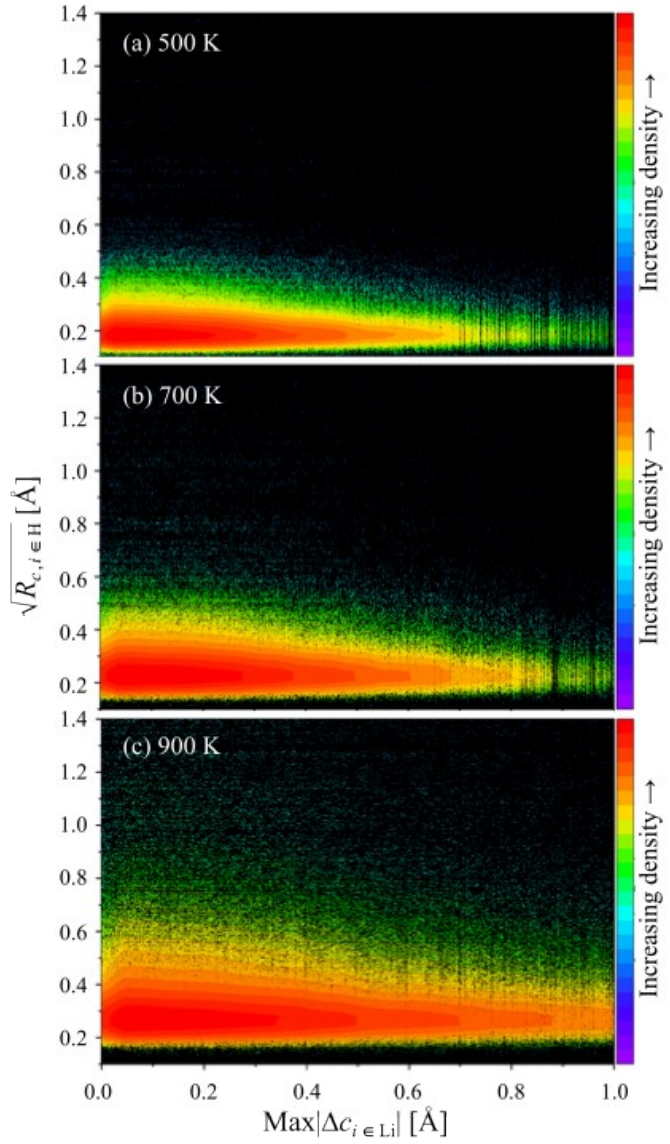

Figure S8. Correlation between Li and H motions. Plot is based on distribution of data points ($x(t)$, $\{y(t)\}$) at every simulation step, where $x(t)$ and $y(t)$ corresponds to the c-axis components of maximum absolute value of Li atom displacements, max|$\Delta c_{i\,\in\,\mathrm{Li}}$|, and root value of rearrangement indicator of H atom, $\sqrt{R_{c,\,i\,\in\,\mathrm{H}}}$, respectively. H atoms connected Li via LiX_6 tetrahedrons are only considered. Rearrangement indicators were calculated by using the time interval of 0.5 ps.